PHYSICAL REVIEW A VOLUME 27, NUMBER 4 APRIL 1983

Diabatic-state treatment of negative-meson moderation and capture. II. Mixtures of hydrogen and helium

James S. Cohen, Richard L. Martin, and W. R. Wadt
Theoretical Division, Los Alamos National Laboratory, University of California, Los Alamos, New Mexico 87545
(Received 24 November 1982)

Slowing-down and capture cross sections have been consistently calculated for μ^-, π^-, K^-, and $\bar{p}$ in collisions with hydrogen and helium atoms and isotopic variants. Capture-energy distributions are determined using the differential-energy-loss cross sections in the laboratory frame. Capture is found to occur predominantly at energies near or below the ionization potential of the target. Ratios of capture on different species are given as a function of the mole fraction of each species present in mixtures. For π^- in a He-H mixture the reduced capture ratio obtained is ~ 0.73, slightly less than the experimental value of 0.92 for the He-H_2 mixture. In contrast with another recent theoretical calculation and in agreement with experimental analysis, it is found that atomic capture of pions in the helium-hydrogen mixture is only slightly nonlinear. It is pointed out that some prior theoretical treatments are in error because of inconsistent calculation of the slowing-down and capture processes and/or subsequent approximate treatment of the energy transport. Use of capture and transfer rates in muon kinetics, e.g., muon-catalyzed fusion, is discussed.

I. INTRODUCTION

The capture of negative mesons in mixtures of hydrogen and helium has been studied experimentally[1,2] and theoretically,[3] but basic questions remain unresolved. This system is of current interest in the rekindled investigation of muon-catalyzed fusion.[4–13] The interpretation of the most recent experiment,[1] which was performed with negative pions using the γ-ray signature of π^0 decay (the π^0 comes from π^- charge exchange with the proton), is complicated by the competition between nuclear capture and transfer to helium following atomic capture of the π^- by hydrogen. Some uncertainty in comparing theory with experiment arises from the fact that the experiments are performed with H_2 molecules, while so far theory has been applied directly only with H atoms. However, many yet-unsettled questions involve the atomic case as well, and the present work will consider the He + H (and isotopically variant) mix. The principal issues, all intimately related, in regard to atomic capture in the mix are the energy at which capture occurs, the He- to H-capture ratio, and the possibility that this capture ratio has a nonlinear dependence on the relative concentrations. The crucial importance of consistent treatment of the slowing-down and capture processes has been emphasized in recent years.[14] Such consistent calculations, using a wide diversity of methods, have been carried out for H atoms[15–17] and He atoms[18] separately, and all show that capture occurs primarily at energies about or below the ionization potential of the target. On the other hand, calculations of the capture cross section alone coupled with use of Rosenberg's[19] slowing-down cross section have predicted capture in much more energetic collisions for both H and He atoms. The present work is the first consistent calculation for the He-H mix.

Several calculations of slowing-down and/or capture cross sections for negative muons by hydrogen atoms have been published. The various results are discussed and compared in Ref. 17, which presents a classical-trajectory Monte Carlo (CTMC) calculation. The CTMC results, which we believe to be the most accurate available at low to moderate energies, are in fairly good agreement with results of the much more economical diabatic-state method[16] at energies below about 200 eV. Since the probability of capture rapidly decreases at energies exceeding the ionization potential, we have chosen to apply the diabatic-state method to the He target as well. Methods used in previous calculations of negative-meson capture by the He atom include the Born approximation by Korenman and Rogovaya,[3] the Coulomb-Born approximation by Haff and Tombrello,[20] and the distorted-wave (DW) method by Cherepkov and Chernysheva.[18] The DW calculation, the best of these descriptions, described the atoms, atomic ion, and ejected electron by Hartree-

Fock wave functions, and the initial and final muon states by Hartree wave functions. The muon initial-state wave function was calculated in the frozen potential of the ground-state atom, and the muon final-state and ejected-electron wave functions were calculated in the frozen potential of the atomic ion. This calculation should be fairly accurate except at low energies where the chosen frozen cores are inappropriate. The DW capture cross section for $\mu^-+\mathrm{He}$ is much smaller than the corresponding Born result except at $E\lesssim 1$ a.u., where the two agree. It may also be noted that at $E\lesssim 1$ a.u. the Born capture cross section for $\mu^-+\mathrm{H}$ is much larger than the CTMC result as well as the adiabatic-ionization (with curved trajectories) result.[17] Adiabatic ionization[21] should be a sensible, though not quantitative, description of $\mu^-+\mathrm{H}$ collisions at low energies. It appears likely that the perturbative methods overestimate the cross section at collision energies below the ionization potential of the target.

The diabatic-state method has been described in detail previously (Ref. 16, referred to as paper I) and so will be only briefly summarized here before proceeding to its results for capture of negative mesons in He-H mixtures.

II. DIABATIC-STATE METHOD

The negative-meson—atom interaction is described in the Born-Oppenheimer framework (i.e., the meson is treated as a heavy particle), but diabatic rather than adiabatic electronic states are employed.[16] The potential-energy curve $V_d(R)$ of the diabatic state ψ_d, unlike the adiabatic potential curve $V_a(R)$, may cross into the electronic continuum even in cases where adiabatic ionization is precluded. At distances R smaller than the crossing into the continuum at R_x the discrete diabatic state has a finite autoionization width, which is given by

$$\Gamma(R)=2\pi\rho_e\,|\,\langle\mathscr{A}\psi_d^+\phi_e\,|\,H-V_d\,|\,\psi_d\rangle\,|^2\,, \tag{1}$$

where ρ_e is the density of states associated with the continuum electron wave function ϕ_e at energy $V_d-V_d^+$, ψ_d^+ is the wave function of the system with one electron removed, and $\mathscr{A}$ is the antisymmetrization operator. The ionic wave function, with potential energy V_d^+, is also calculated in the Born-Oppenheimer approximation, using the same core orbitals as in ψ_d. In practice, we avoid direct evaluation of continuum integrals by discretizing the continuum and utilizing Stieltjes moment theory.[22]

It is now convenient to formulate the collision problem in terms of the complex potential

$$W(R)=V_d(R)-\frac{i}{2}\Gamma(R)\,. \tag{2}$$

The scattering in this potential is treated by the impact-parameter method with quasiclassical trajectories. For a collision at relative energy $E_{\mathrm{c.m.}}$ and impact parameter b, the probability of ionization is obtained as the solution of the first-order differential equation

$$\frac{dp(R)}{dR}=\lambda\left[\frac{m}{2E_{\mathrm{c.m.}}}\right]^{1/2}\left[1-\frac{b^2}{R^2}-\frac{V_d(R)}{E_{\mathrm{c.m.}}}\right]^{-1/2}\times\Gamma(R)[1-p(R)]\,, \tag{3}$$

where m is the reduced mass. On the trajectory, R goes from ∞ to R_{cl} (with $\lambda=-1$), then from R_{cl} to ∞ (with $\lambda=+1$), where the classical turning point R_{cl} satisfies

$$E_{\mathrm{c.m.}}-V_d(R_{\mathrm{cl}})-\frac{b^2E_{\mathrm{c.m.}}}{R_{\mathrm{cl}}^2}=0\,. \tag{4}$$

The two values of $p(R)$ are denoted $p_{\mathrm{in}}(R)$ and $p_{\mathrm{out}}(R)$. The doubly differential cross section for an energy loss ϵ in a collision at impact parameter b is given by

$$\frac{d^2\sigma(E_{\mathrm{c.m.}},\epsilon,b)}{d\epsilon\,db}=2\pi b\int_{R_{\mathrm{cl}}}^{R_x}f(\epsilon,R)\frac{d}{dR}[-p_{\mathrm{in}}(R)+p_{\mathrm{out}}(R)]\times\left|\frac{d\epsilon_0(R)}{dR}\right|^{-1}dR\,. \tag{5}$$

The energy losses are distributed about the energy

$$\epsilon_0(R)=V_d(R)-V_d^+(R)+I_a\,, \tag{6}$$

where I_a is the ionization potential of the target atom.[23] The distribution function $f(\epsilon,R)$ is not completely determined by the theoretical formulation. In paper I a Lorentzian distribution (with width Γ) was assumed. Subsequently, the CTMC calculation[17] has shown directly that the energy distribution is more nearly exponential. Hence we now use an exponential distribution (with width Γ),

$$f(\epsilon,R)=C(R)\exp[-(2\ln 2)\,|\,\epsilon-\epsilon_0(R)\,|\,/\Gamma(R)]\,, \tag{7}$$

where $C(R)$ is a normalization constant.

The differential energy-loss cross section is given by

$$\frac{d\sigma(E_{\mathrm{c.m.}},\epsilon)}{d\epsilon}=\int_0^\infty\frac{d\sigma(E_{\mathrm{c.m.}},\epsilon,b)}{d\epsilon\,db}db\,. \tag{8}$$

If $\epsilon > E_{\text{c.m.}}$, the negative meson is captured; hence we can calculate the capture cross section

$$\sigma_{\text{capt}}(E_{\text{c.m.}}) = \int_{E_{\text{c.m.}}}^{\infty} \frac{d\sigma(E_{\text{c.m.}},\epsilon)}{d\epsilon} d\epsilon \tag{9}$$

and the slowing-down cross section

$$\sigma_{\text{slow}}(E_{\text{c.m.}}) = \int_{0}^{E_{\text{c.m.}}} \frac{d\sigma(E_{\text{c.m.}},\epsilon)}{d\epsilon} d\epsilon \,. \tag{10}$$

The total ionization cross section can be obtained as the sum of σ_{capt} and σ_{slow}, or more directly by

$$\sigma(E_{\text{c.m.}}) = 2\pi \int_0^{\infty} p_{\text{out}}(R \to \infty) b \, db \,. \tag{11}$$

III. INTERACTION POTENTIALS AND CROSS SECTIONS

The potentials for the interactions of negative mesons with H and He atoms are shown in Figs. 1 and 2. The same curves apply independent of the meson mass since the calculations are done in the Born-Oppenheimer approximation. The potential curves shown are the electronic energies, the attractive meson-nucleus Coulomb term having been subtracted out. The results for the H atom, from paper I,[16] show that the diabatic curve crosses into the continuum at $R_x \simeq 1.86a_0$ as compared to the adiabatic critical distance[21] of $R_c \simeq 0.64a_0$. Qualitatively, πR_x^2 is a better estimate of the effective low-energy stopping cross section than is the much smaller πR_c^2. Of course, in any system where the negative ion, formed in the adiabatic united-atom limit, is bound, adiabatic ionization is not possible at all. This is the case for $\mu^- + \text{He}$ whose interaction potentials are shown in Fig. 2 (the united-atom limit is H^-). The $\mu^- + \text{He}$ calculations were done with a basis set similar to that used for $\mu^- + \text{H}$, $20-s$, $20-p$, and $20-d$ even-tempered Gaussian functions on the He atom (the d functions were omitted in the Stieltjes-moment-theory calculation of Γ). In the diabatic calculation of V_d^+ the same $1s$ orbital appropriate to neutral He was imposed on He^+; hence V_d^+ does not quite approach V_a^+ as $R \to \infty$. The diabatic crossing for $\mu^- + \text{He}$ occurs at $R \simeq 0.96a_0$, a smaller distance than the $\mu^- + \text{H}$ diabatic crossing. On the other hand, the width Γ is larger for He than for H so it is perhaps not immediately obvious which will present the larger cross section.

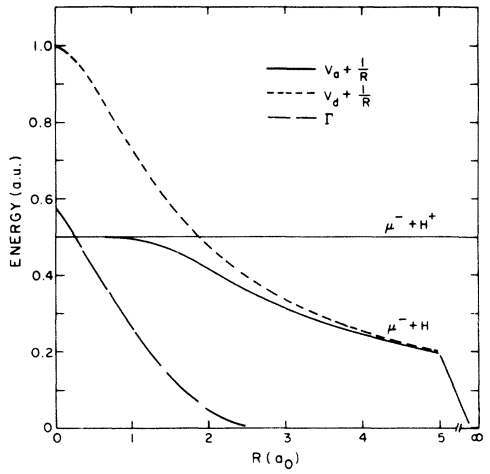

FIG. 1. Electronic potential energies (excluding muon-nucleus Coulomb attraction) of $\mu^- + \text{H}$ and $\mu^- + \text{H}^+$ interactions. Adiabatic energies (solid curves), diabatic energies (short-dashed curves), and the ionization width of the diabatic state (long-dashed curve) are shown. Since the negative meson is fixed in the Born-Oppenheimer approximation, the same curves apply to any other "heavy" particle of charge -1 (i.e., π^-, K^-, and $\bar{p}$). Unit of energy is 1 a.u. ($=27.21$ eV) and the unit of distance is $1a_0$ ($=0.529\,18 \times 10^{-8}$ cm).

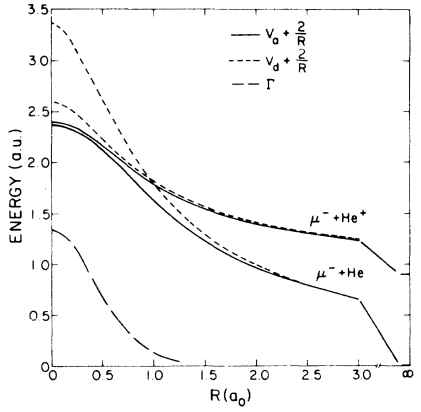

FIG. 2. Electronic potential energies of $\mu^- + \text{He}$ and $\mu^- + \text{He}^+$. See caption of Fig. 1 for other details.

In the cross-section calculations the adiabatic potential curve was used at $R > 4a_0$ (well outside R_x) and the diabatic curve at $R < 2.5a_0$, with smooth interpolation in between. The only effect of the adiabatic curve is in the determination of long-range barriers in the effective potential $V(R) + (b/R)^2 E_{\text{c.m.}}$, which reduce the cross section at very low collision energies. The capture and slowing-down cross sections for $\mu^- + \text{H}$ and $\mu^- + \text{He}$ are shown in Figs. 3 and 4, respectively, as a function of laboratory scattering energy

$$E_{\text{lab}} = (1+\gamma) E_{\text{c.m.}} \,, \tag{12}$$

where γ is the ratio of the meson mass to target mass. Clearly, the capture cross sections decrease rapidly at relative collision energies exceeding the

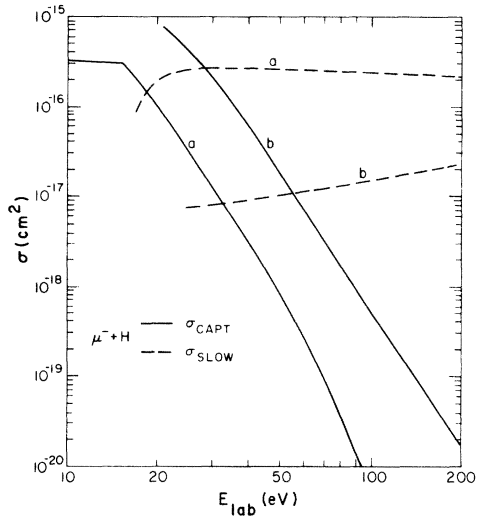

FIG. 3. Slowing-down cross sections σ_{slow} (dashed curves) and capture cross sections σ_{capt} (solid curves) for μ^-+H. a, Present calculations; b, values from Ref. 3 (σ_{slow} from Ref. 19).

ionization potential of the target; i.e., the electron generally escapes with a kinetic energy smaller than 1 a.u. as the result of a low-energy collision. At relative collision energies below the ionization potential, the capture cross section increases relatively slowly as the collision energy decreases, owing to trajectory deflection by the Coulomb attraction to the nucleus. The Born-approximation capture cross sections,[3] which have also been used to describe the He-H mixture, are shown for comparison in Figs. 3 and 4. The present capture cross sections fall off somewhat faster than the Born values at $E_{c.m.} > I_a$ and, more importantly, are much smaller. On the other hand, the present capture cross section for He does not fall off quite as rapidly as does the DW result,[18] but the two are comparable in magnitude. Both perturbative results, the Born and DW approximations, give much larger capture cross sections than the present calculations at $E_{c.m.} < I_a$, even though the Born approximation does not account for trajectory curvature. It is also interesting to observe that the change in the capture cross section at energies near the ionization potential is much more gradual in the perturbative approaches than in the present calculation and in the presumably more accurate CTMC calculation (the total ionization cross sections are still quite smooth in all the calculations).

The slowing-down cross sections, which are equally important for determining capture-energy distributions, are also shown in Figs. 3 and 4. The present result is somewhat smaller than the DW cross section, but both are much larger than the value of Rosenberg[19] which has been used in conjunction with the Born approximation to capture.[3] Roughly speaking, one may expect capture to occur at energies where the capture and slowing-down cross sections are comparable. More precisely, it is the differential energy-loss cross section which is required in the calculation of capture distributions. The part of this cross section reflecting energy imparted to the ionized target electron is denoted $d\sigma/d\epsilon$ and determined by Eq. (8). Its values are

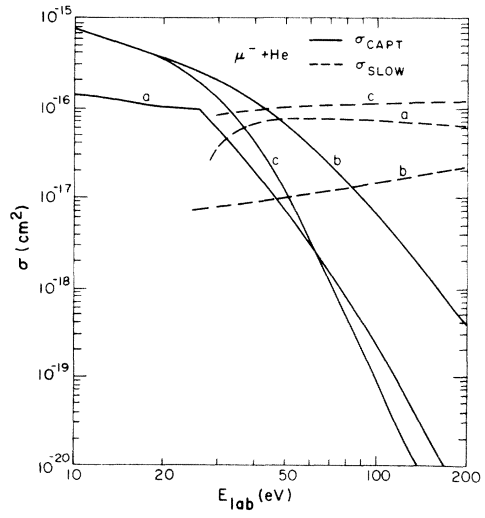

FIG. 4. Slowing-down cross sections σ_{slow} (dashed curves) and capture cross sections σ_{capt} (solid curves) for μ^-+He. a, Present calculations; b, values from Ref. 3 (σ_{slow} from Ref. 19); and c, results from Ref. 18.

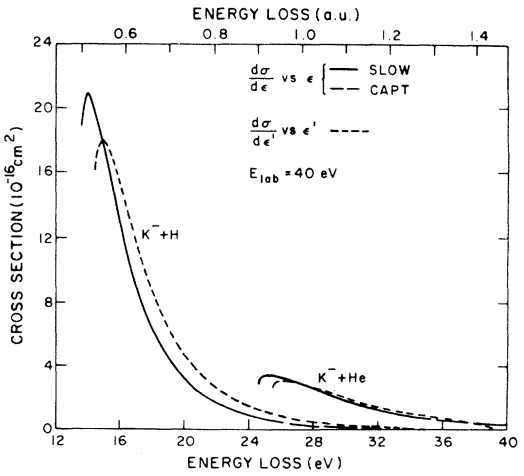

FIG. 5. Differential energy-loss cross sections for K^-+He and K^-+H in the c.m. frame ($d\sigma_{slow}/d\epsilon$, solid curve; $d\sigma_{capt}/d\epsilon$, long-dashed curve) and in the laboratory frame ($d\sigma_{slow}/d\epsilon'$, short-dashed curve). Collision energy is $E_{lab}=40$ eV, or $E_{c.m.}=35.3$ for K^-+He and 26.2 eV for K^-+H.

shown in Fig. 5 for collisions of negative kaons with H and He atoms.

There is an additional contribution to energy loss which is due to the momentum imparted to the target atom. Previous work has suggested that the component of this energy transfer resulting from elastic scattering is negligible.[18] However, it is clear that transfer of kinetic energy in nonelastic scattering must also be accompanied by transfer of kinetic energy to the target nucleus (assumed to be initially stationary in the laboratory frame). The latter energy loss has often been neglected but can be significant especially for the heavier projectiles (K^- and $\bar{p}$) and for capture at very low energies. Simple consideration of conservation of linear momentum shows that the total energy loss (in the laboratory frame) is given by

$$\epsilon' \simeq \frac{\epsilon}{\gamma+1} + \frac{2\gamma E_{\rm lab}}{(\gamma+1)^2} + \frac{2\gamma^2 E_{\rm lab}\sin^2\theta}{(\gamma+1)^2} - \frac{2\gamma E_{\rm lab}}{(\gamma+1)^2}\left[1-\frac{(\gamma+1)\epsilon}{E_{\rm lab}}\right]^{1/2} \times \left[1-\frac{\gamma^2\sin^2\theta}{1-\frac{(\gamma+1)\epsilon}{E_{\rm lab}}}\right]\cos\theta\,, \tag{13}$$

where θ is the laboratory deflection angle of the projectile. In this expression the momentum of the electron has been neglected since it is quite small, and the electron is expected to be emitted nearly isotropically (in the c.m. frame) in any event. Consistent with the neglect of elastic scattering, the deflection angle in inelastic scattering will also be neglected. This deflection angle is not given by the usual diabatic-state treatment and would involve a considerably greater computational effort. (For each $E_{\rm c.m.}$ and b, a longer trajectory would have to be integrated and branched to the final state at a number of points where ionization is possible. The contribution of deflection could more sensibly be checked in the CTMC calculation where exact three-dimensional dynamics is performed.) The ratio ϵ'/ϵ is shown in Fig. 6 for $\theta=0$. Neglecting deflection the total differential-energy-loss cross section $d\sigma/d\epsilon'$ can be obtained simply from $d\sigma/d\epsilon$ using the relation

$$\epsilon \simeq (\gamma+1)\epsilon' - 2\gamma E_{\rm lab}\left[1-\left[1-\frac{\epsilon'}{E_{\rm lab}}\right]^{1/2}\right]. \tag{14}$$

The values of $d\sigma/d\epsilon'$ for K^-+H and K^-+He are also shown in Fig. 5 for comparison with $d\sigma/d\epsilon$. Note that capture occurs when $\epsilon > E_{\rm c.m.}$, or equivalently $\epsilon' > [(2\gamma+1)/(\gamma+1)^2]E_{\rm lab}$. Also note that ϵ has a minimum value $\epsilon_{\rm min}$, which for capture

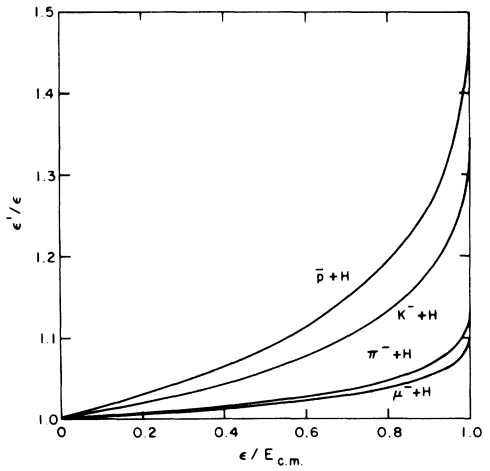

FIG. 6. Approximate ratio of energy loss ϵ' in the laboratory frame to energy loss ϵ in the c.m. frame as a function of $\epsilon/E_{\rm c.m.}$ for μ^-, π^-, K^-, and $\bar{p}$ colliding with H atoms.

is equal to the target ionization potential. Consequently, in the absence of elastic scattering, the lowest laboratory energy at which a free negative meson can occur is

$$E_{\rm lab}^{\rm min} = [\gamma^2/(\gamma+1)]\epsilon_{\rm min}\,. \tag{15}$$

Elastic scattering will fill this void to some extent (of course, the target atoms are not exactly stationary in the laboratory frame, as assumed, either).

IV. CAPTURE DISTRIBUTIONS AND DISCUSSION

The capture distributions are conveniently determined via the arrival probability density[24] $F_{\rm arr}(E_{\rm lab})$, which is defined such that the probability of a negative meson arriving (sometime during its history before capture) in an energy interval $dE_{\rm lab}$ at $E_{\rm lab}$ is given by $F_{\rm arr}(E_{\rm lab})dE_{\rm lab}$. The arrival function satisfies the integral equation

$$F_{\rm arr}(E_{\rm lab}) = \int_0^\infty B_{\rm free}(E_{\rm lab}+\epsilon',\epsilon') \times F_{\rm arr}(E_{\rm lab}+\epsilon')d\epsilon'\,, \tag{16}$$

where the branching ratio for free-free collisions is

$$B_{\rm free}(E_{\rm lab},\epsilon') = \frac{\sum_i a_i \Theta\left[\frac{2\gamma_i+1}{(\gamma_i+1)^2}E_{\rm lab}-\epsilon'\right]\frac{d\sigma_i(E_{\rm lab},\epsilon')}{d\epsilon'}}{\sum_i a_i\sigma_i(E_{\rm lab})}\,. \tag{17}$$

Here a_i is the fraction of species i in the mixture,

and $\Theta(x)=1$ for $x \geq 0$ and 0 otherwise. Equation (16) is solved numerically by starting with a normalized uniform distribution in some "high" energy range. With the present cross sections an initial distribution between 9 and 10 a.u. (much lower, of course, than the actual initial meson energies) was found to be sufficient to eliminate any dependence of $F_{\rm arr}$, in the energy range where capture occurs, on the initial conditions. In terms of the solution of Eq. (16), the normalized capture probability density for species i is then given by

$$F^{(i)}_{\rm capt}(E_{\rm lab})=\int_0^\infty B^{(i)}_{\rm capt}(E_{\rm lab},\epsilon')F_{\rm arr}(E_{\rm lab})d\epsilon' , \tag{18}$$

where the capture branching ratio is

$$B^{(i)}_{\rm capt}(E_{\rm lab},\epsilon') = \frac{a_i\Theta\left[\epsilon'-\frac{2\gamma_i+1}{(\gamma_i+1)^2}E_{\rm lab}\right]\frac{d\sigma_i(E_{\rm lab},\epsilon')}{d\epsilon'}}{\sum_i a_i\sigma_i(E_{\rm lab})} . \tag{19}$$

Finally, the probability of capture by species i is obtained,

$$W_i=\int_0^\infty F^{(i)}_{\rm capt}(E_{\rm lab})dE_{\rm lab} . \tag{20}$$

In the preceding paragraph we have been somewhat cavalier with the quantity ϵ'. Recall that ϵ' was defined as the energy loss of the negative meson in the laboratory frame and so is rather arbitrary in the case of capture. Actually, all that is required is a mapping $\epsilon'\rightarrow\epsilon$ which is smooth at the boundary between free-free and free-bound collisions. For this purpose we used

$$\epsilon=\left[\left[\epsilon'-\frac{2\gamma+1}{(\gamma+1)^2}E_{\rm lab}\right]^3+\frac{E^3_{\rm lab}}{(\gamma+1)^3}\right]^{1/3} \tag{21}$$

for $\epsilon'>[(2\gamma+1)/(\gamma+1)^2]E_{\rm lab}$. It is easily verified that this expression joins smoothly with Eq. (14) at $\epsilon'=[(2\gamma+1)/(\gamma+1)^2]E_{\rm lab}$. This connection allows the convenience of not having to bother with any frame transformation in solving Eq. (16). The binding energy of the captured negative meson is given by

$$E_b=\epsilon-E_{\rm c.m.}=\epsilon-\frac{E_{\rm lab}}{1+\gamma} ; \tag{22}$$

clearly, this is *not* the same as $\epsilon'-E_{\rm lab}$ since the c.m. of the mesonic atom must remain in motion after capture.

The energy distributions are shown in Fig. 7 for capture of negative muons in pure H and in pure He. The result for H differs from that in paper I at very low energies since the calculation in I was done in the c.m. frame. It is more proper to do the calculation in the laboratory frame, especially for mixtures which will be considered below. The present results are compared with those of Korenman and Rogovaya (KR)[3] and Cherepkov and Chernysheva (CC)[18] in Fig. 7. The results of KR show capture occurring at much higher energies than do either the present results or those of CC. The capture energies obtained by Haff and Tombrello[20] (not shown) are even higher than those of KR (half the muons captured by $\sim$75 eV in H and by $\sim$200 eV in He). The earliest calculation of KR (1975) found capture in H mainly at still higher energies ($>$200 eV). The high capture energies are due more to their use of inconsistent capture and slowing-down cross sections (both used the stopping power of Rosenberg[19]) than to the use of the Born approximation for capture. We may note that elastic and (nonionizing) inelastic scattering, which we (and the other calculations) neglect, can only reduce the energy at which capture occurs.

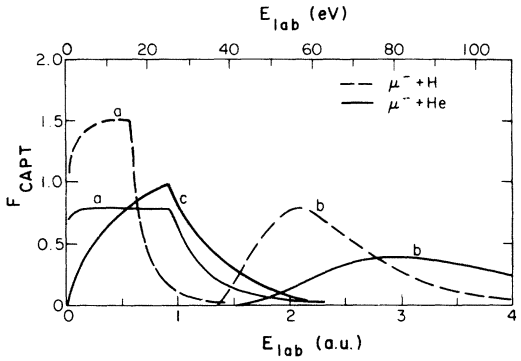

FIG. 7. Energy distributions of muon capture in pure He (solid curves) and pure H (dashed curves). a, Present results; b, results from Ref. 3; and c, results from Ref. 18.

The energy distribution of CC for μ^- capture by He is in fair agreement with the present calculation, although it does fall off at energies immediately below the He ionization potential in contrast to the present distribution which is relatively flat below the ionization potential down to a quite low energy. This falloff appears to be due to the approximate method used by CC to determine the arrival function rather than their actual cross sections. They assume for this purpose that

$$\frac{d\sigma_{\rm slow}(E,\epsilon)}{d\epsilon}\simeq\sigma_{\rm slow}(E)\delta(\epsilon-I_a) \tag{23}$$

and consequently approximate Eq. (16) by

$$F_{\rm arr}(E-I_a)=F_{\rm arr}(E)\left[\frac{\sigma_{\rm slow}(E)}{\sigma_{\rm slow}(E)+\sigma_{\rm capt}(E)}\right]. \tag{24}$$

Hence, in effect, energy losses greater than I_a are allowed in the case of capture but not in the case of slowing down. This inconsistency causes a decrease in $F_{\rm capt}(E)$ starting immediately below I_a. In fact, if the energy losses decrease as the collision energy decreases, which is generally the case, $F_{\rm capt}(E)$ may peak below I_a. We believe that if the cross sections of CC were used in Eq. (16) the resulting distribution would be in even better agreement with ours. This agreement might at first seem a little surprising considering that the capture cross section of CC is significantly larger than ours at $E<I_a$. The explanation is that in both calculations it is assumed that only capture occurs at $E<I_a$ and thus the magnitude of $\sigma_{\rm capt}$ here has no effect on $F_{\rm capt}$. However, the magnitude of the cross section at $E<I_a$ will have an important effect on mixtures whose components have different values of I_a. The approximation presumed in Eq. (24) could cause most serious errors in predicting capture ratios.

Two examples of capture-energy distributions in mixtures are shown in Fig. 8. The mixture is comprised of equal amounts of He and H, and the distribution of captures on each atom is shown for μ^- and K^- mesons. The relative values of the H and He capture distributions largely reflect the ratio of the respective capture cross sections, and deviation of their shapes from that of the capture profiles of the pure species (shown in Fig. 7) reflects the energy dependence of this ratio. The structure at very low energies, which is most apparent in Fig. 8 for capture of K^-, arises from the different values of $E_{\rm lab}^{\rm min}$ [see Eq. (15)] for the two different target atoms. The probability of capture by a given species W_i, obtained by integrating the capture-energy distribution according to Eq. (20), is shown in Fig. 9 for He_μ formation in He-H mixtures. According to the present calculations, the fraction of muons captured by He is somewhat less than the mole fraction of He in the mixture of He and H atoms.

Perhaps more instructive than the capture probability itself is the *reduced capture ratio* $(W_1/W_2)/(a_1/a_2)$. A nonconstant value of this ratio signifies a nonlinear dependence of capture probability on the relative abundances of the species. The reduced capture ratios are shown in Fig. 10 for muons in He-H, He-D, and He-T mixes. A mild nonlinearity is exhibited. The reduced capture ratios at three different relative abundances are also given in Table I for muons in these and other mixes, as well as for π^-, K^-, and $\bar{p}$ in the He-H mix. The nonlinearity of the capture probability is most easily interpreted in terms of the arrival function, as discussed by Leon.[24] If the arrival function is *constant*, then the reduced capture ratio is simply the ratio of the capture cross sections integrated over energy; i.e., it does not matter that capture occurs at different energies for the two species. On the other hand, if the arrival function increases as the particles slow down, then capture at lower energies is favored, and conversely. Nonlinearity may result if the arrival function depends on the relative concentrations of the species in the mix. One might think that owing to capture the arrival function always decreases as the energy decreases, but such is not the case. In a consistent calculation there is a relation between slowing down and capture indicated by the differential energy-loss cross section; that is, $d\sigma(E_{\rm c.m.},\epsilon)/d\epsilon$ is continuous at $\epsilon=E_{\rm c.m.}$. Actually, at very low energies the arrival function in the labo-

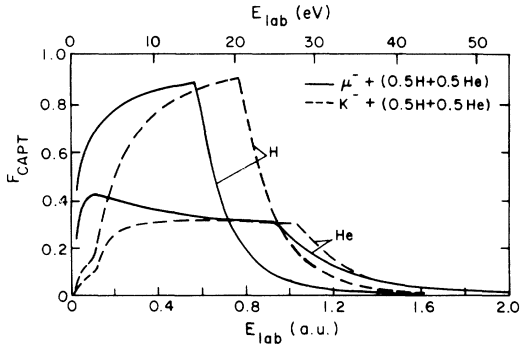

FIG. 8. Energy distributions of muon (solid curves) and kaon (dashed curves) capture by He and H in a mixture comprised of equal mole fractions of He and H.

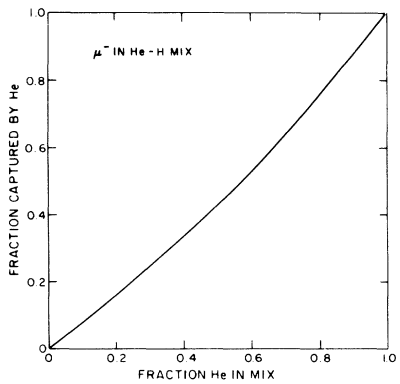

FIG. 9. Fraction of muons captured by He as a function of the mole fraction of He in a mixture of He and H.

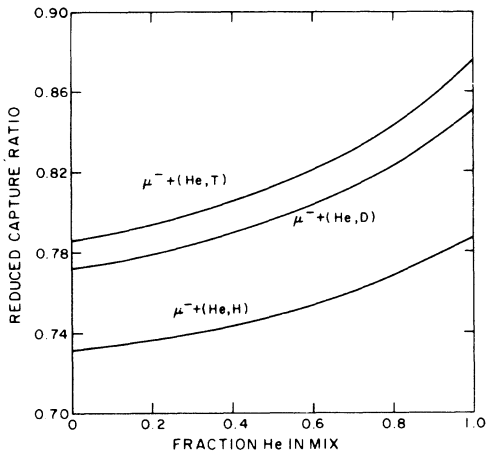

FIG. 10. Reduced capture ratios [e.g., $(W_{He}/W_H)/(a_{He}/a_H)$] for muon capture in mixtures of helium (^{4}He) with hydrogen (protium), deuterium, and tritium. Departures from constant values signify nonlinear capture.

ratory frame does decrease (at least, if elastic scattering is neglected) owing to the momentum transfer which must accompany ionization, but not necessarily as a result of capture. At higher energies the shapes of the arrival functions in the two frames do not differ greatly. Setting aside the effect of momentum transfer by considering the arrival function in the c.m. frame, then, as Leon clearly points out, $dF_{capt}/dE<0$ if energy losses decrease as E decreases, and conversely. Note that it is the shape and not the magnitude of the energy-loss cross section which is relevant; i.e.,

$$\frac{1}{\sigma(E)}\frac{d\sigma(E,\epsilon)}{d\epsilon} \tag{25}$$

should be compared at different energies E.

In the present calculations energy losses in the c.m. frame decrease slightly as the particles slow down in the energy range where capture may occur. Consequently, the arrival function in the laboratory frame has a maximum and is rather flat at $E_{lab}\gtrsim 0.5$ a.u. The reduced capture ratio is given approximately by the ratio of the capture cross sections integrated over energy, and the nonlinearity is slight. What nonlinearity there is comes from the fact that the decrease of energy losses as the particles slow down is greater for H than for He targets, so the arrival function for pure H has its maximum at lower energy than does the arrival function for pure He. Hence if the arrival function is determined primarily by H, as is the case in a mixture of mostly H, capture at low energy, i.e., by H, is favored. The result is a reduced capture ratio (He relative to H) which increases as the mole fraction of He increases. It is important to understand that this behavior is the result of the collision-energy dependence of the energy-loss cross section and not merely the result of captures on He occurring at higher energies than captures on H.

Capture at different energies is a necessary although not sufficient condition for nonlinearity. For the heavier particles π^-, K^-, and $\bar{p}$ in the He-H mix, this condition is less well satisfied than for μ^-, and the nonlinearity can be seen to be decreasing in Table I. The laboratory collision energy at which capture first occurs with high probability is given by $(\gamma_i+1)I_a^{(i)}$ for species i; for the He-H mix these energies (in eV) are 25.3 and 15.1 for μ^-, 25.5 and 15.6 for π^-, 27.8 and 20.8 for K^-, and 30.8 and 27.2 for $\bar{p}$. The effect for μ^- and K^- can be seen in Fig. 8.

For isotopic mixes these "thresholds" differ because of the different reduced masses (the difference in ionization potentials is negligible); e.g., the energies are 14.4 and 15.1 for μ^- in the D-H mix. This difference yields a nonunity reduced capture ratio (see Table I), but, as already emphasized, is not suf-

TABLE I. Reduced capture ratios $(W_1/W_2)/(a_1/a_2)$.[a]

	$a_1=0.01$, $a_2=0.99$	$a_1=a_2=0.5$	$a_1=0.99$, $a_2=0.01$
μ^-+(He,H)	0.732	0.749	0.788
π^-+(He,H)	0.711	0.726	0.759
K^-+(He,H)	0.555	0.558	0.564
$\bar{p}$+(He,H)	0.431	0.433	0.434
μ^-+(He,D)	0.772	0.796	0.851
μ^-+(He,T)	0.786	0.812	0.873
μ^-+(D,H)	0.936	0.937	0.937
μ^-+(T,D)	0.978	0.978	0.978
μ^-+(He,^{3}He)	0.987	0.987	0.987

[a]Subscripts 1 and 2 refer to the species of the mixture in the order listed in column 1.

ficient to guarantee nonlinearity. In fact, the energy-loss shapes for μ^-+H and μ^-+D are similar, and the nonlinearity is negligible. We note that if these calculations had been done in the c.m. system, the reduced capture ratios obtained for the isotopic mixes would be virtually unity.

V. COMPARISON WITH EXPERIMENT

We have consistently calculated slowing-down and capture cross sections, capture-energy distributions, and capture ratios for μ^-, π^-, K^-, and $\bar{p}$ in He-H (and isotopically variant) mixtures. Thus the initial atomic capture is characterized. Available experimental observations have been made, however, after a time during which some transfer from the lighter to heavier nucleus may have occurred. While it has been verified both experimentally[2,25,26] and theoretically[27] that transfer from ground-state mesonic hydrogen to helium occurs at a very slow rate, this hindrance does not apply to excited states (it has been estimated[27] that transfer from H_μ to He is appreciable for levels $n \gtrsim 5$). In the most thorough experimental study to date, Petrukhin and Suvorov[1] found that the observed probability of nuclear capture by hydrogen of a π^- meson stopped in the He-H_2 mixture is accurately fit by the form

$$W_H^{\rm obs}=P_H q \ , \tag{26}$$

where

$$P_H=(1+AC)^{-1} \tag{27}$$

is interpreted as the probability of initial atomic capture by hydrogen, and

$$q=(1+A'C^{4/3})^{-1} \tag{28}$$

is interpreted as the probability of pion transfer from hydrogen to helium not occurring. Letting C be the ratio of *atomic* number densities, i.e.,

$$C=n_{\rm He}/n_H=0.5n_{\rm He}/n_{H_2} \ , \tag{29}$$

they obtained

$$A=A'=1.84\pm0.09 \ .$$

Another measurement[1,28] gave $A=1.72\pm0.13$ indirectly. Hence the net result is strongly nonlinear, but Petrukhin and Suvorov predict that the initial atomic capture is linear in agreement with earlier less accurate experiments[2] and consistent with the present weak nonlinearity shown in Fig. 10 and Table I.

The most sensible quantitative comparison between capture experiments (with H_2) and theory (with H) is made by using equal number densities of H_2 and H. This is the case because undoubtedly the *slow* negative meson about to be captured "sees" the molecular orbital and not the separate atoms in the molecule. (The situation of capture may be contrasted with that of deactivation of H_μ^*, for example, where the small neutral H_μ^* is expected to "see" each nucleus separately.[29] In this case it is proper to count H_2 as two H atoms.) The present results then give $A \simeq 1.46$ in Eq. (27) for pions in the He-H_2 mixture. (Note that A would be a factor of 2 smaller in both the experimental and theoretical cases if C were defined as the ratio of mole fractions a_1/a_2.) The agreement with experiment is quite satisfactory. *A priori,* it is not possible to predict reliably whether H or H_2 should be more effective at capturing negative mesons. On the one hand, H_2 has the larger ionization potential, thus favoring H_2. On the other hand, adiabatic ionization is not possible with H_2, implying that H_2 may have the smaller cross section. The latter relation is mildly suggested by the difference between the present and experimental values of A. In any event, the Z-scaling law is not valid.

Korenman and Rogovaya[3] have challenged the experimental analysis made by Petrukhin and Suvorov. On the basis of their theoretical treatment of the He-H mix (Born approximation for capture mated with Rosenberg's stopping power) they predict a large nonlinearity in the initial atomic-capture rate and assert that the experimental results can be interpreted on this basis alone with no transfer from hydrogen to helium occurring. We have suggested in Sec. IV that this large nonlinearity is due to their inconsistent treatment of slowing down and capture, and, in fact, such a large nonlinearity would be difficult to obtain in atomic capture. In this regard we emphasize the importance of solving Eq. (16) for the distribution of free particles accurately in the laboratory frame. We believe that our results lend credance to the experimental analysis of Petrukhin and Suvorov. If this conclusion is correct, then in most applications, e.g., to the kinetics of muon-catalyzed fusion, the transfer of negative mesons after initial capture must be taken into account. To do this fully would require knowledge of yet-undetermined cross sections for deactivation of H_μ^* and transfer from various levels of H_μ^* to He. A formula of the type in Eqs. (26)—(28) may be adequate, but the effective transfer probability q depends on the specific reaction observed (charge exchange with the nucleus in the aforementioned pion experiment). In the case of muon-catalyzed fusion the situation is not entirely clear. The formation rate for the $dt\mu$ molecule via the recently verified resonant mechanism[8,9(d)] may be comparable to the muon-transfer rate from excited states of muonic hydrogen

to helium.[27] Since reaction of the muon with the nucleus is negligible, it is possible that transfer of muons is still important at lower excited states than for pions. Until more specific data is available on the kinetics of muon-catalyzed fusion, it is probably reasonable to use the effective capture ratio measured for pions.

ACKNOWLEDGMENTS

We are grateful to Professor L.I. Ponomarev for suggesting this problem and to Dr. M. Leon for many beneficial discussions. This work was performed under the auspices of the U.S. Department of Energy.

[1]V. I. Petrukhin and V. M. Suvorov, Zh. Eksp. Teor. Fiz. 70, 1145 (1976) [Sov. Phys.—JETP 43, 595 (1976)]; V. I. Petrukhin, Yu. D. Prokoshkin, and V. M. Suvorov, *ibid.* 55, 2173 (1968) [*ibid.* 28, 1151 (1969)].

[2]O. A. Zaimidoroga *et al.*, Zh. Eksp. Teor. Fiz. 44, 1852 (1963) [Sov. Phys.—JETP 17, 1246 (1963)].

[3]G. Ya. Korenman and S. I. Rogovaya, Radiat. Eff. 46, 189 (1980); J. Phys. B 13, 641 (1980); Yad. Fiz. 22, 754 (1975) [Sov. J. Nucl. Phys. 22, 389 (1975)].

[4]S. S. Gershtein and L. I. Ponomarev, in *Muon Physics,* edited by V. W. Hughes and C. S. Wu (Academic, New York, 1975), Vol. III, p. 141, and references therein.

[5]S. S. Gershtein and L. I. Ponomarev, Phys. Lett. 72B, 80 (1977); S. S. Gershtein *et al.*, Zh. Eksp. Teor. Fiz. 78, 2099 (1980) [Sov. Phys.—JETP 51, 1053 (1980)].

[6]J. Rafelski, in *Exotic Atoms '79,* edited by K. Crowe, J. Duclos, G. Fiorentini, and G. Torelli (Plenum, New York, 1980), p. 177.

[7]L. Bracci and G. Fiorentini, Nucl. Phys. A364, 383 (1981); Nature (London) 297, 134 (1982); Phys. Rep. 86, 169 (1982).

[8]S. I. Vinitskii, Zh. Eksp. Teor. Fiz. 74, 849 (1978) [Sov. Phys.—JETP 47, 444 (1978)].

[9](a) V. M. Bystritskii *et al.*, Zh. Eksp. Teor. Fiz. 70, 1167 (1976) [Sov. Phys.—JETP 43, 606 (1976)]; (b) 71, 1680 (1976) [44, 881 (1976)]; (c) 76, 460 (1979) [49, 232 (1979)]; (d) 80, 1700 (1981) [53, 877 (1981)]; (e) Phys. Lett. 94B, 476 (1980).

[10]L. N. Bogdanova, Yad. Fiz. 34, 1191 (1981) [Sov. J. Nucl. Phys. 34, 662 (1981)].

[11]Yu. V. Petrov, Nature (London) 285, 466 (1980).

[12]S. Tesch, Kernenergie 25, 97 (1982).

[13]S. G. Lie and A. A. Harms, Nucl. Sci. Eng. 80, 124 (1982).

[14]See, for example, M. Leon, in *Exotic Atoms '79,* Ref. 6, p. 141.

[15]T. J. Baird, Ph.D. thesis, Rensselaer Polytechnic Institute, 1976 (unpublished) and Los Alamos Report No. LA-6619-T (unpublished).

[16]J. S. Cohen, R. L. Martin, and W. R. Wadt, Phys. Rev. A 24, 33 (1981). Referred to as paper I.

[17]J. S. Cohen, Phys. Rev. A 27, 167 (1983).

[18]N. A. Cherepkov and L. V. Chernysheva, Yad. Fiz. 32, 709 (1980) [Sov. J. Nucl. Phys. 32, 366 (1980)].

[19]R. L. Rosenberg, Philos. Mag. 40, 759 (1949).

[20]P. K. Haff and T. A. Tombrello, Ann. Phys. (N.Y.) 86, 178 (1974).

[21]A. S. Wightman, Phys. Rev. 77, 521 (1950).

[22]A. U. Hazi, J. Phys. B 11, L259 (1978).

[23]Here, ϵ is defined as the energy loss (in the c.m. system); in Ref. 16, ϵ was defined as the kinetic energy of the ejected electron (i.e., I_a less than the present definition).

[24]M. Leon, Phys. Rev. A 17, 2112 (1978).

[25]M. Schiff, Nuovo Cimento 22, 66 (1961).

[26]A. Placci, E. Zavattini, A. Bertin, and A. Vitale, Nuovo Cimento 52A, 1274 (1967).

[27]A. V. Matveenko and L. I. Ponomarev, Zh. Eksp. Teor. Fiz. 63, 48 (1972) [Sov. Phys.—JETP 36, 24 (1973)].

[28]Yu. G. Budyashov, V. G. Zinov, A. D. Konin, and A. I. Mukhin, Yad. Fiz. 5, 830 (1967) [Sov. J. Nucl. Phys. 5, 589 (1967)].

[29]J. S. Cohen and J. N. Bardsley, Phys. Rev. A 23, 46 (1981).